Saudi Pharmaceutical Journal 30 (2022) 454–461

Contents lists available at ScienceDirect

Saudi Pharmaceutical Journal

journal homepage: www.sciencedirect.com

Original article

Formulation and characterization of tobramycin-chitosan nanoparticles coated with zinc oxide nanoparticles

Nusaiba.K. Al-nemrawi [a,*], Rami Q. Alkhatib [b], Hadeel Ayyad [c], Nid''A Alshraiedeh [a]

[a] Department of Pharmaceutical Technology, Faculty of Pharmacy, Jordan University of Science and Technology, Jordan
[b] Department of Biotechnology and Genetic Engineering, Faculty of Science and Art, Jordan University of Science and Technology, Jordan
[c] Department of Applied Biological Sciences, Faculty of Science and Art, Jordan University of Science and Technology, Jordan

ARTICLE INFO

Article history:
Received 21 October 2021
Accepted 20 January 2022
Available online 31 January 2022

Keywords:
Tobramycin
Nanoparticles
Ionic gelation
TPP
Zinc oxide
Bacterial resistance

ABSTRACT

Herein we describe the preparation, characterization and the antibacterial effect of Tobramycin-chitosan nanoparticles (TOB-CS NPs) coated with zinc oxide nanoparticles (ZnO NPs). Four formulations of TOB-CS NPs (A-D) were prepared to study the effect of experimental variables on the NPs behavior. Two formulations of ZnO NPs were prepared using the solvothermal and the precipitation methods (ZnO_1 and ZnO_2), and then characterized. TOB-CS NPs (Formula d) was coated with the ZnO_1. Moreover, the antibacterial activity of TOB-CS NPs, ZnO NPs and the coated nanoparticles against *S. aureus* and *E. coli* was examined. Changing the variables in preparing TOB-CS NPs resulting in variabilities in sizes (297.6–1116.3 nm), charges (+8.29–+39.00 mV), entrapment (51.95–90.60%). Further, TOB release was sustained over four days. ZnO NPs have sizes of 47.44 and 394.4 nm and charges of −62.3 and 89.4 mV when prepared by solvothermal and precipitation technique, respectively. Coated TOB-CS NPs had a size of 342 nm, a charge of +4.39 and released 100 μg/ mL of the drug after four days. The antimicrobial activity of TOB-CS NPs was lower than free TOB against *S. aureus* and *E. coli*. The coated NPs showed higher antimicrobial effect in comparison to formula D and ZnO_1. In conclusion, coating TOB-CS NPs with ZnO NPs exhibited a great antibacterial effect that may be sustained for days.

1. Introduction

In the last decades, the resistance to known antibiotics quickly developed and become one of the major public health concerns (Lister et al., 2009). Even though, old antimicrobial agents saved many lives in the last century, new strategies are required to overcome the emerging bacterial resistance. The development of novel drug delivery systems is one of the promising approaches that is under investigation to limit bacterial resistance (Medina and Pieper, 2016; Kashi et al., 2012). Using new antibacterial agents such as metal-based nanoparticles are also gaining attention to kill resistance bacteria (Sondi and Salopek-Sondi, 2004).

Many polymers have been used to prepare nanoparticles that are loaded with well-known or new antibiotics either to target bacterial cells or to control drugs' release. Chitosan (CS) is one of the mostly used polymers which is partially deacetylated chitin derivative. It has a pKa around 6, which is related to the presence of the amine groups, which give CS its exceptional properties (Szymańska and Winnicka, 2015). Chitosan displays many attractive properties that allowed it to be the focus of medical and pharmaceutical industry; its water soluble, biocompatible, non-toxic, non-immunogenic and biodegradable (Kumari and Rath, 2014). In the last decades, chitosan nanoparticles (CS NPs) have been prepared and studied to be used in drug delivery (Grenha, 2012).

Many antibiotics have been loaded in CS NPs such as tetracycline, gentamycin, ciprofloxacin, rifampicin, tobramycin (TOB) and many others (El-Alfy et al., 2020; Khan et al., 2021; Scolari et al., 2020). TOB has been loaded in CS NPs to control its release. Other researchers loaded TOB in NPs that are decorated with CS to get advantages of CS physicochemical properties (Al-Nemrawi et al., 2018b). TOB is a broad spectrum aminoglycoside antibiotic that is used to treat bacterial infections (Laxer et al., 1975). It works either by blocking protein synthesis from the ribosomes, or by causing damage in the bacterial membrane (Davis, 1987).

* Corresponding author.
E-mail address: nknemrawi@just.edu.jo (N.K. Al-nemrawi).

Peer review under responsibility of King Saud University.

Production and hosting by Elsevier

https://doi.org/10.1016/j.jsps.2022.01.016

Using new pharmaceutical entities have been used to solve or limit bacterial resistance. These entities include prodrugs, peptides, proteins, natural materials and nanoparticles(Sekhri, n.d.; S. Moore et al., 2017). Many metallic nanoparticles showed great activity against several bacterial species with multi drug-resistance. For example, copper oxide, zinc oxide, ferric oxide and silver nanoparticles inhibited different bacterial strains. Zinc oxide nanoparticles (ZnO NPs) have the largest antibacterial activity among all studied metals (Azam et al., 2012; Sanpui et al., 2008). The exact mechanisms of ZnO NPs as antimicrobial is not known, but two mechanisms were suggested to explain this effect. The first one involves the production of reactive oxygen species (ROS), which results in oxidative stress that damages the bacterial membrane. The second mechanism implies mechanical damage of the microorganism cellular wall, where ZnO NPs damage the bacterial cell wall. This is usually followed by the accumulation of ZnO NPs in the cell inhibiting some bacterial metabolic activities (Janaki et al., 2015; Motelica et al., 2020).

ZnO NPs ranging from 50 to 500 nm were found to be effective against several types of bacteria. It also has been widely used as an anti-inflammatory agent by inhibiting some cytokines (Siddiqi et al., 2018). ZnO NPs are synthesized by different methods, including precipitation, hydrothermal, solvothermal, and microemulsion method (Kumar et al., 2013).

Herein, chitosan nanoparticles were used to load TOB (TOB-CS NPs) in order to control its release. Then, these nanoparticles were coated with ZnO NPs to enhance their antibacterial effect. The combination of two or more antimicrobial agents is one of the oldest protocols that is used to enhance the antimicrobial effect. The combination of CS and ZnO NPs have been employed in the food and textile industry long time ago to kill bacteria (AbdElhady, 2012; La et al., 2021; Yadav et al., 2021). Recently, researchers start to think of using this combination as a medication (Gutha et al., 2017; Yusof et al., 2019).

In this study, CS NPs loaded with TOB were prepared and characterized. The effect of the formulation parameters was assessed, and the antimicrobial efficacy of the best formulation was examined in vitro. In addition, ZnO NPs were prepared by different methods and characterized, and their antimicrobial efficacy was assessed in vitro. Finally, the best formulation of TOB-CS NPs was coated with the best formulation of ZnO NPs and characterized, and its antimicrobial activity was examined. This study aimed to elaborate the effect of loading TOB in CS NPS on its release and its antibacterial activity. Moreover, coating these NPs with ZnO NPs was invistigated.

2. Materials and methods

2.1. Materials

TOB was purchased from Acros Organics (New Jersy, USA), low molecular weight chitosan (50 kD, 90% DDA), 2,4-dinitrofluorobenzene, zinc nitrate and ammonium carbonate were purchased from Sigma Aldrich (Reykjavik, Iceland). Tripolyphosphate was purchased from AZ chem (Oragine,China). All other chemicals and reagents used in this study were of analytical grade.

2.2. Synthesis of tobramycin-chitosan nanoparticles

A modified ionic gelation method developed in our lab was used to prepare four tobramycin-chitosan nanoparticles (TOB-CS NPs) (Al-Nemrawi et al., 2018a). An aqueous solution, referred to as Phase 1, was prepared by dissolving CS and TOB in 40 mL of a 0.2% acetic acid solution. The solution pH was adjusted to 5.0 ± 0.05 using sodium hydroxide and the solution was stirred overnight. Then, filtered through a 0.45 μm syringe filter (Next Advance, USA), and heated to 60 °C in a water bath for 10 min.

In a different beaker, the second phase, referred to as Phase 2, was prepared by dissolving TPP in 20 mL of HPLC water. Then, the solution was filtered through a 0.45 μm syringe filter and cooled to −4°C.

Phase 2 was added to the heated Phase 1 dropwise at a rate of 1 mL/min under continuous stirring at 700 rpm. The resulting dispersion stirred and then centrifuged at 10,000 rpm for 30 min. Then, the nanoparticles were washed twice with distilled water. Finally, the sample was freeze-dried for 24 h at −80 °C to obtain the nanoparticles.

Formula A and B were prepared to get the weight ratios of 1:2:2 and 1:5:5 of Chitosan: TOB: TPP, respectively. Formula C and D were prepared using the same procedure used to prepare Formula A and B, except that TOB was added to Phase 2 rather than to Phase 1. The weight ratio of Chitosan: TOB: TPP of formula C and D were 1:2:2 and 1:5:5, respectively. All powdered samples were kept in a tightly closed containers for future studies. Table 1 shows the components of each formulation in each phase.

2.3. Characterization of tobramycin-chitosan nanoparticles

The mean particles size (PS), the polydispersity index (PDI) and the zeta potential (ZP) of the NPs were determined using a Zetasizer nano ZS90 instrument (Malvern Instruments, Malvern, UK) at 25℃ using dynamic light scattering (DLS) in triplicate. The zeta potentials were determined by placing samples after dispersing them in distilled water at 25 ∘C in disposable zeta cells. The electrophoretic mobility between the electrodes was converted to a zeta potential, depending on the Smoluchowski equation. All measurements were performed in triplicate.

The morphologies of TOB-CS NPs were investigated using Scanning Electron Microscopy (SEM) (Thermo scientific, Darmstadt, Germany). The samples were coated with a golden film before analysis.

The Fourier-transform infrared (FTIR) spectrum of CS, TOB and TOB-CS NPs were compared using Shimadzu FTIR instrument (Kyoto, Japan) with a high-performance diamond single-bounce ATR accessory. The samples were studied in the range 400–4000 cm $^{-1}$, with a resolution of 4 cm and were scanned 64 scans per spectrum.

2.4. Drug entrapment efficiency

In preparing the NPs, the supernatant was collected and used to detect the amount of free TOB. Then, the encapsulated amount of TOB was calculated by subtracting the free amount of TOB from the total amount used. The drug entrapment efficiency (EE) was found by measuring the free amount of TOB that was not entrapped in the NPs in relation to the total amount of TOB used in the preparation. The EE was measured as follow:

$$EE = \frac{Total\ \ tobramycin - Free\ \ tobramycin}{Total\ \ tobramycin} \times 100\%$$

TOB concentration was measured using HPLC-UV method described by Russ et al with minor modifications (Russ et al., 1998). The samples were pre-column derivatized by 2,4-Dinitroflurobenzene reagent and Tris (hydroxymethyl) aminomethane reagent. C_{18} column (5 μm, 4.6 × 250 mm) was used separate the samples at 25℃, and the λ_{max} was set at 365 nm. To prepare the mobile phase, 2.0 g of tris (hydroxymethy1) aminomethane were dissolved in 800 mL of water, and 20 mL of 1 N sulfuric acid was added. Then, 1200 mL of acetonitrile was added to complete the volume to 2 L. The flow rate was set at 1.0 mL/min.

Table 1
The amounts of each ingredient used in preparing the four formulations of TOB-CS NPs (A, B, C & D) in each phase.

Formulations								
	A		B		C		D	
Phase 1 (40 mL)	CS TOB	20 mg 40 mg	CS TOB	20 mg 100 mg	CS	20 mg	CS	20 mg
Phase 2 (20 mL)	TPP	40 mg	TPP	100 mg	TPP TOB	40 mg 40 mg	TPP TOB	100 mg 100 mg

2.5. In vitro drug release

TOB release from chitosan nanoparticles was investigated in vitro. TOB-CS NPs equivalent to 3 mg of TOB from each formula were redispersed in 3 mL of phosphate buffer saline (PBS) solution (pH = 7.4 ± 0.05) and placed in a dialysis bag with a molecular cut-off ~12–14 KDa. Then the bags were tied, placed in a beaker, and soaked in 12 mL of PBS solution. The beakers were kept in a water bath (Daihan Scientific, Korea) with continuous agitation at 100 rpm at 37 °C. At certain time points, 1 mL of the dissolution medium was withdrawn and replaced with 1 mL of fresh PBS solution. The amount of TOB released into the dissolution medium was measured by the HPLC-UV method mentioned previously. All measurements were performed in triplicate and the percentage of TOB released was plotted against time.

2.6. Synthesis of zinc oxide nanoparticles

ZnO NPs were prepared by two methods: The precipitation method (ZnO_2) and the solvothermal technique (ZnO_1). In the precipitation method, zinc nitrate was first dissolved in deionized water and added to ammonium carbonate solution in a volume ratio of 1.5:1 to interact and give ZnO NPs that precipitate. After that, the precipitate was purified by washing with deionized water and heated for six hours in an oven at 90 °C. The obtained powder was kept in the furnace at 500 °C for four hours. Finally, the particles were freeze dried and the powdered sample was kept in a tightly closed container for future studies.

In the solvothermal technique, ethanolic solution of NAOH was dropped into another ethanolic solution of zinc acetate that was kept at 70 °C in water path. The mixture was kept at 70 °C for 1 hr, and then, the mixture was centrifuged for 3 min at 2500 rpm. The precipitate was washed by ethanol and centrifuged again at 2500 rpm several times. Finally, the particles were freeze-dried and the powdered sample was kept in a tightly closed container for future studies.

2.7. Characterization of zinc oxide nanoparticles

Both FTIR and zeta sizer were used to identify and characterize ZnO NPs under the same conditions mentioned previously in characterizing CS NPs. X-ray diffractometer (Rigaku, Ultima IV) (XRD) was used to characterize ZnO NPs with a diffraction angle of 2θ, ranging from 10 to 80°. Powdered ZnO NPs were dispersed on the quartz sample holder and placed on goniometer to record the diffraction pattern at all possible angle of diffraction using DTEX detector with a scanning rate of 5° per minute.

2.8. Coating of TOB-CS NPs with ZnO NPs

The best TOB-CS NPs (Formula D) was coated with the best ZnO NPs formulation. TOB-CS NPs were dispersed in 10 mL of 1% acetic acid solution and stirred for 30 min. Then, ZnO NPs powder was added, and the mixture was stirred for another 30 min. The dispersion was centrifuged 10,000 rpm for 30 min and washed several times with distilled water. The particles were freeze-dried and the powdered sample was kept in tightly closed container for future studies.

2.9. Characterization of the coated TOB-CS NPs

To characterize the coated NPs, the PS, PDI and ZP were measured. Further, the coated particles were examined using FTIR, SEM and XRD and compared to TOB-CS NPs and ZnO NPs. Finally, the in vitro drug release from the coated particles was explored and compared to TOB releases from TOB-CS NPs.

2.10. Antimicrobial activity test

Two-fold broth dilution method was used to determine the minimum inhibitory concentration (MIC) of TOB, TOB-CS NPs, ZnO NPs and the coated TOB-CS NPs. The samples were studied against *Escherichia coli* (ATCC 25922) as a gram negative bacteria and *Staphyloccocus aureus* (ATCC 29215) as a gram positive bacteria. Each bacterial strain was grown on Muller Hinton agar overnight at 37 °C. The following day, each type of bacteria was suspended in Muller Hinton broth (MHB), and adjusted to have an optical density (OD_{600}) of $2x10^7$ and $1x10^5$cfu/mL for *E. coli* and *S. aureus,* respectively. Solutions of each sample were prepared in sterile MHB. Then, 100 μL of the bacterial suspension was added to all the wells and incubated at 37 °C for 24 h. A negative control that consists of pure broth, and a positive control that consists of broth and bacteria, were included in each plate. In addition, the following concentrations were used to determine the MIC (62.5, 125, 250, 500, 1000, and 2000 μg/ml). After the 24 hr of incubation, all plates were read using ELISA reader. The MIC was determined as the lowest concentration at which no growth was visually observed in the inoculated wells. All plates were studied in triplicates.

3. Results and discussion

3.1. Characterization of tobramycin-chitosan nanoparticles

The PS, PDI, ZP and EE of the NPs are summarized in Table 2. Formula D exhibited the smallest size followed by formula B then formula A and finally formula C. Even though the sizes of the particles are somehow large, they still can be considered. Polymeric nanoparticle prepared using chitosan reaching 1000 nm were reported previously to be used to load antimicrobial drugs and to control their release(Abruzzo et al., 2021; Al-Nemrawi et al., 2018b; Nguyen et al., 2017). The PDI values of all formulations indicate monodispersity of the samples with the best uniformity for formula D followed by formula B then formula A and finally formula C. From the results, we can notice that the amount of TPP used affects the sizes of CS NPs, where the higher the concentrations of TPP used in preparing CS NPs results in larger NPs (Jonassen et al., 2012). In this study, formula D showed the smallest size and the best uniformity. Moreover, the size of the particles

Table 2
The size PDI, zeta potential and EE values of TOB-CS NPs.

Formulation	Size (nm)	PDI	Zeta potential (mV)	EE (%)
A	826.80 ± 48.99	0.570 ± 0.058	+28.20 ± 1.76	51.95 ± 1.21
B	690.90 ± 26.60	0.355 ± 0.078	+39.00 ± 2.93	90.60 ± 2.48
C	1116.30 ± 260.60	0.711 ± 0.124	+8.29 ± 0.36	87.43 ± 2.07
D	297.60 ± 3.67	0.249 ± 0.014	+13.10 ± 0.36	58.76 ± 1.30
ZnO_1	47.44 ± 1.93	0.533 ± 0.036	−62.30 ± 0.44	NA
ZnO_2	394.40 ± 6.41	0.600 ± 0.061	−89.40 ± 1.41	NA
Coated TOB-CS NPs	324.07 ± 23.60	0.613 ± 0.086	+4.39 ± 1.22	56.76 ± 1.64

of formula D is lower than the sizes of TOB-CS NPs prepared by other investigators (Vaezifar et al., 2013).

All NPs carried positive charges, which can be explained by the free amine groups of chitosan that get protonated in water. Differences in the surface charges between the formulas may be related to the extent of crosslinking between the negatively charged TPP with the positive amino groups of chitosan (Al-Nemrawi et al., 2018a).

In this study, the EE of TOB in all formulations was very high and more than 50%. The EE varied between the four formulations, but had higher values in comparison to nanoparticles prepared using the same method by other researchers (Sobhani et al., 2017). The morphology of TOB-CS NPs was investigated. All formulas showed spherical NPs as represented in Fig. 1.

The FTIR spectrums of TOB, CS and TOB-CS NPs. TOB spectrum shows two sharp peaks at 1345 cm^{-1} and 1583 cm^{-1} related NH bending (Fig. 2). Another one broad band is seen around 3000 cm^{-1}, which is related to the OH and NH groups. Peaks in the same range were reported by other researchers (Junejo et al., 2019).

The spectrum of chitosan showed a characteristic broad band at 3447 cm^{-1} related to NH_2 and OH groups stretching. The band at 2880 cm^{-1} corresponds to CH stretching vibration of CH_2 groups. Also, the peak at 1654 cm^{-1} corresponds to the NH_2 group bending vibrations. Further, a band corresponding to NH_2 stretching at 1064 cm^{-1} was noticed (Nguyen et al., 2020 ; Lawrie et al., 2007). The spectrum of TOB-CS NPs is different from those of CS and TOB. Many peaks appeared, disappeared, or shifted, which prove the interaction between TOB and CS in the nanoparticles. A new peak in the spectrum of the NPs appears at 2124 cm^{-1} that is related to intermolecular OH stretching("IR Spectrum Table," n. d.). Further, the peak at 1591 cm^{-1} in the spectrum of TOB disappeared. Additionally, the two peaks at 1345 cm^{-1} and 1583 cm^{-1} in the spectrum of TOB are shifted to lower values. Moreover, the band at 2880 cm^{-1} and 1654 cm^{-1} that appeared in CS's spectrum disappeared. The bands at 1064 cm^{-1} in CS's spectrum and at 1018 in TOB's spectrum become weak in the nanoparticles' spectrum.

3.2. In vitro drug release

TOB release from the four formulations was determined over 4 days. There was no release of the drug from formulas A and B after 4 days. In both formulations, TPP and TOB were added to the same phase. This may result in a strong ionic interaction between the positively charged TOB and the negatively charged TPP, which prevent the drug release. On the other hand, TOB was added to the phase that contain CS (both are positively charged), which may be limited TOB interaction with TPP and allow the drug release during the release study. Because of this withholding behavior of the drug, formulations A and B were excluded from the study and were not considered further.

The release from formulas C and D showed two phases release profile (Fig. 3). The drug release showed two stages: an initial burst stage followed by a sustained drug release stage. Such behavior was noticed in other chitosan nanoparticles, where the initial rapid drug release was explained by the residuals of the drug adsorbed to the surface of chitosan nanoparticles (Al-Nemrawi and Dave, 2016). The sustained release of TOB can be attributed to the diffusion of TOB through the chitosan NPs. Formula D showed faster release of the drug in comparison to formula C, which may be related to the lower particle size and lower PDI of formula D. The smaller the NPs size, the larger is the surface-to-volume ratio, which will cause large amount of the drug to be located near the surface, leading to a faster drug release at the beginning (Rizvi and Saleh, 2018). Because of its better physicochemical properties and release behavior, Formula D was chosen to be coated with ZnO NPs.

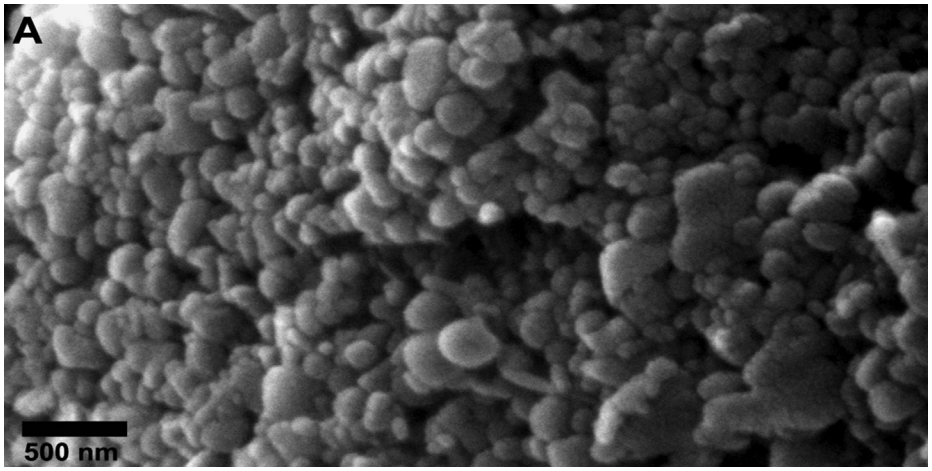

Fig. 1. Scanning electron micrograph images of TOB-CS NPs.

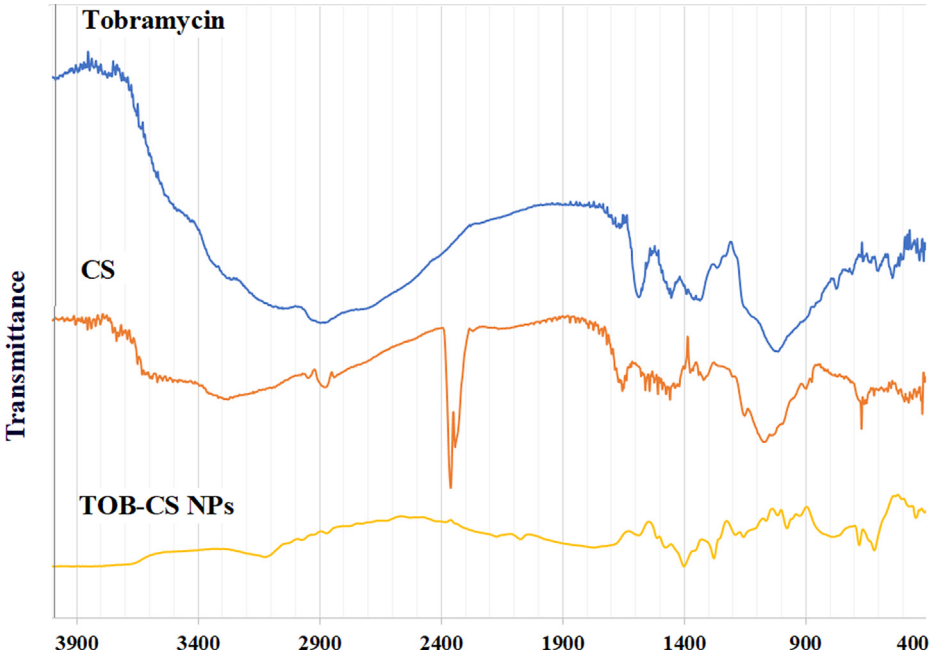

Fig. 2. FT-IR spectrum of tobramycin (TOB), chitosan (CS) and TOB-CS NPs (formula D).

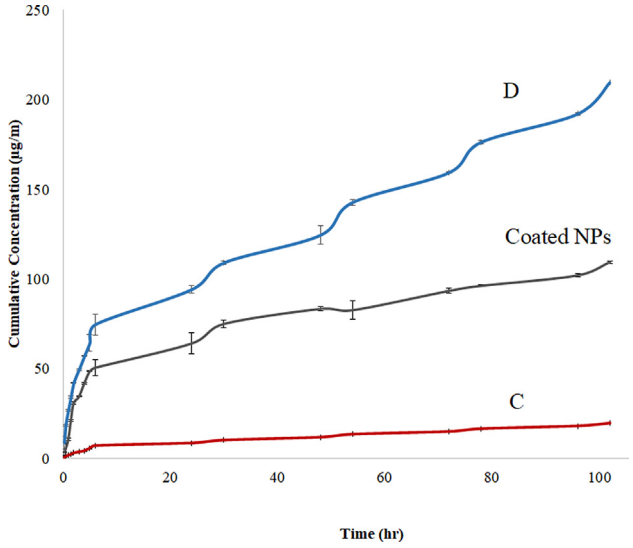

Fig. 3. Cumulative release profiles of TOB loaded in CS NPs in phosphate buffered saline (pH = 7.4) at 37 °C.

3.3. Characterization of zinc oxide nanoparticles

The PS of the ZnO NPs prepared in this work are summarized in Table 1. The particles prepared by solvothermal method showed smaller sizes in comparison to the particles prepared by the precipitation method. The charges of all ZnO NPs are negative regardless the method of preparation. The low PDI of ZnO NPs indicates acceptable monodispersity of both preparations. When analyzed by XRD, ZnO NPs showed crystalline structures as shown in Fig. 4. The peaks at 2θ = 31.5, 34.18, 36, 56.28, and 62.6° that can be seen in Fig. 4 were reported previously as the characteristic peaks of hexagonal lattice structure of ZnO NPs (Mohan and Renjanadevi, 2016). The FTIR spectra of ZnO NPs showed peaks near 512 cm^{-1} and 550 cm^{-1} and a peak at 457 cm^{-1}, which indicate the formation of ZnO NPs. Finally, because of their lower sizes and charges, ZnO_1 NPs were chosen to be used to coat TOB-CS NPs.

3.4. Characterization of the coated TOB-CS NPs

In this work, the best formulation of TOB-CS NPs (Formula D) was coated with the best formulation of ZnO NPs (ZnO_1). TOB-CS NPs and ZnO NPs were dispersed in acetic acid solution to allow the interaction between them as described previously by other researchers (Al-Naamani et al., 2016; Bharathi et al., 2019). The resulted system showed higher size, higher PDI and lower ZP in comparison to the uncoated TOB-CS NPs as summarized in Table 2. The higher PS could be related to the accumulation of ZnO NPs on the surface of TOB-CS NPs, but it seems that this accumulation was not regular, which was reflected by the PDI values. The lower values of ZP may be a result of the ionic interaction between the positively charged TOB-CS NPs and the negatively charged ZnO NPs.

The coated TOB-CS NPs were examined using FTIR and XRD and compared to TOB-CS NPs and ZnO NPs. FTIR spectra are shown in Fig. 5. The figure shows that ZnO NPs have a peak at 3124 cm^{-1} corresponds to the OH stretching vibration of H_2O and a peak at 1645 cm^{-1} may be related to the OH bending vibration. Also, the peak at 1400 cm^{-1} may be related to the H–O–H bending vibration or the absorbed CO_2 bands. Finally, the band in the range of 530–420 cm^{-1} refers to the stretching mode of ZnO (Nguyen et al., 2020; Raja et al., 2014).

Compared to the spectrums of TOB-CS NPs, new bands from 509 to 412 cm^{-1} referring to the ZnO NPs stretching appears in the spectrum of coated nanoparticles. Additionally, the peak in chitosan at 3124 cm^{-1} that is related to the OH stretching is broader and shifted to 3115 cm^{-1} in the coated nanoparticles. This indicates the strong intermolecular hydrogen bonding interaction between that ZnO NPs and TOB-CS NPs ("Infrared Spectroscopy Absorption Table," 2014).

The XRD spectrum of the physical mixture is shown in Fig. 5. CS showed two peaks at 11 and 20°. The coated NPs showed the characteristic peaks of ZnO NPs, as well as the two peaks of TOB-CS NPs.

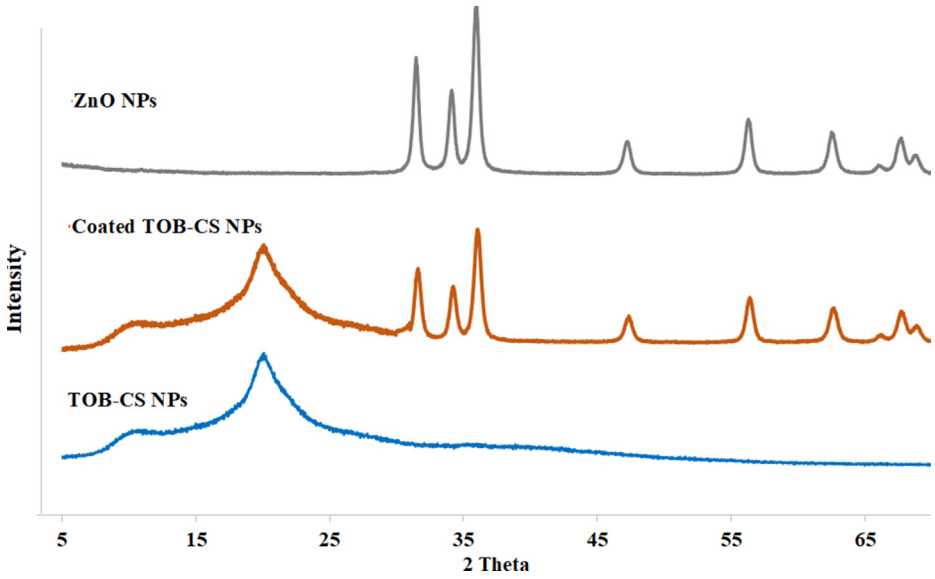

Fig. 4. XRD spectrum of TOB-CS NPs (formula D), ZnO_1 and the coated nanoparticles.

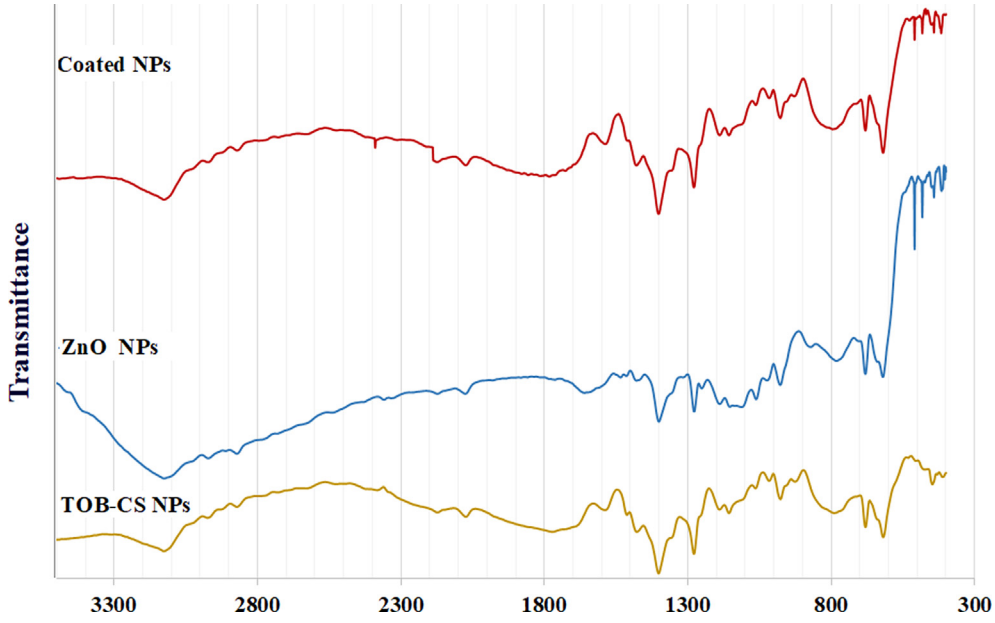

Fig. 5. FT-IR spectrum of TOB-CS NPs (formula D), ZnO_1 and the coated nanoparticles.

3.5. Antimicrobial activity testing

The antibacterial activity of TOB, TOB-CS NPs (formula D), ZnO NPs, and the coated TOB-CS NPs were tested against *E. coli* and *S. aureus*. The results are shown in Table 3 and Table 4, respectively. Our results showed that TOB had antibacterial activity against the two strains of bacteria, with the highest effect against *E. coli* followed by *S. aureus*. Based on the literature, the MIC value for pure TOB against *E. coli* (ATCC 25922) was around 1.42 μg/mL. However, there is no MIC data found on *S. aureus* (ATCC 29215), meanwhile the MIC value for *S. aureus* (ATCC 25923) was 0.20 μg/mL (Shadomy and Kirchoff, 1972). In this current study, MIC values for TOB against *E. coli and S. aureus* were 1.95 and 3.9 μg/mL, respectively. When TOB was loaded into chitosan nanoparticles, the MIC values increased (Table 3). Even though, the amount of TOB loaded in TOB-CS NPs and the amount of pure TOB tested are equivalent,

Table 3
The antibacterial activity of TOB, TOB-Cs NPs, ZnO NPs and the physical mixture of TOB-CS NPs/ZnO NPs.

Microorganism	MIC (μg/mL)			
	TOB	TOB-CS	ZnO NPs	Coated TOB-CS NPs
S. aureus	3.90 ± 0.04	15.60 ± 0.09	50.00 ± 3.01	10.70 ± 0.08
E. coli	1.95 ± 0.03	11.30 ± 0.12	100.00 ± 3.40	8.40 ± 0.11

Table 4
The minimum inhibitory concentration (MIC) of ZNO NPs for *E. coli* and S. *aureus*. (+) indicates killing activity, meanwhile (-) indicates no killing activity has been seen and bacteria were able to grow.

Microorganism	ZNO NPs Conc. (μg/mL)					
	2000	1000	500	250	125	62.5
E. Coli	+	+	–	–	–	–
S. aureus	+	+	+	–	–	–

the gradual release of TOB from the nanoparticles may explain lower antimicrobial activity of the nanoparticles (Al-Nemrawi et al., 2018b; Cheow et al., 2010). It is worth to mention that CS, as a part of TOB-CS NPs, was reported to have antimicrobial activity by itself (Radulescu et al., 2015).

ZnO NPs had low activity against *E. coli and S. aureus* with MIC values of 100 and 50 μg/mL, respectively (Table 3). The higher sensitivity of gram-negative than gram-positive bacteria toward ZnO NPs may be related to the bacterial cell wall structure. The outer membrane of gram-positive bacteria is composed of structural lipopolysaccharides that make the cell wall impermeable and more resistance to foreign substances including antibacterial agents (Beveridge, 1999; Lüderitz et al., 1982).

The detailed activity of ZnO NPs against *E. coli and S. aureus* is shown in Table 4. In literature, the MIC values of ZnO NPs against *S. aureus* highly varied from 4 to 3000 μg/mL, but in general it was very low in comparison to that of TOB-CS NPs. The same low and variable MIC values were reported for ZnO NPs against *E. coli.* These MIC values ranged between 30 and 2500 μg/mL (Azizi-Lalabadi et al., 2019; Nazoori and Kariminik, 2018). This huge variability in ZnO NPs antibacterial activity may be related to the method of its preparation, as well as its characteristics. It was reported that ZnO NPs in the size range of 50–500 nm had a bactericidal effect on different bacterial strains (Siddiqi et al., 2018). Other researchers demonstrated that there is a size-dependent antibacterial effect of ZnO NPs (Raghupathi et al., 2011).

Finally, the MIC values of coated TOB-CS NPs was less than that of uncoated NPs. Therefore, we can conclude that coating TOB-CS NPs with ZnO NPs may enhance their antimicrobial activity. The combination of ZnO NPs and TOB was reported to enhance the antimicrobial effect of both agents (Khan et al., 2021). Therefore, it is expected that coating nanoparticles, loaded with TOB, with ZnO NPs to have similar effect. As we mentioned, ZnO NPs generate oxidative stress in the cellular microbiome that ultimately damage the cell membrane proteins and DNA, leading to cell death (Azam et al., 2012; Siddiqi et al., 2018). On the other hand, TOB that is released from TOB-CS NPs functions by binding to the bacterial 30S and 50S ribosome and prevents the formation of the 70S complex. This prevents mRNA translation into proteins, and consequently lead to cell death (Laxer et al., 1975). Because of these different modes of action, the coated nanoparticles showed better antimicrobial efficacy than ZNO NPs and TOB-CS NPs.

4. Conclusion

In conclusion, TOB-CS NPs with an entrapment efficacy reaching 90% with small sizes, monodispersed and positively charged were prepared successfully. The experimental conditions and the amounts of the materials affect the nanoparticles properties and the drug release from them. In addition, TOB-CS NPs was found to be effective against both *E. coli* and *S. aureus.* ZnO NPs were successfully prepared by both solvothermal and precipitation method. The NPs prepared by the solvothermal technique have lower sizes and charges in comparison to those prepared by the precipitation technique. ZnO NPs showed antimicrobial activity against both *E. coli* and *S. aureus*. Coating TOB-CS NPs with ZnO NPs enlarged the particles' size and lower their charges. Further, it slower the drug release and enhances the antimicrobial activity against the studied species. Finally, we can conclude that loading TOB in CS NPs and coating them with ZnO NPs may enhance the antibacterial activity and control it over along time.

Declaration of Competing Interest

The authors declare that they have no known competing financial interests or personal relationships that could have appeared to influence the work reported in this paper.

Acknowledgement

The authors thank the Deanship of Research at Jordan University of Science and Technology (JUST) for their generous fund (Proposal Number: 348/2019).

References

AbdElhady, M.M., 2012. Preparation and characterization of chitosan/zinc oxide nanoparticles for imparting antimicrobial and UV protection to cotton fabric. Int. J. Carbohyd. Chem. 2012, 1–6. https://doi.org/10.1155/2012/840591.

Abruzzo, A., Giordani, B., Miti, A., Vitali, B., Zuccheri, G., Cerchiara, T., Luppi, B., Bigucci, F., 2021. Mucoadhesive and mucopenetrating chitosan nanoparticles for glycopeptide antibiotic administration. Int. J. Pharm. 606, 120874. https://doi.org/10.1016/j.ijpharm.2021.120874.

Al-Naamani, L., Dobretsov, S., Dutta, J., 2016. Chitosan-zinc oxide nanoparticle composite coating for active food packaging applications. Innovat. Food Sci. Emerg. Technol. 38, 231–237. https://doi.org/10.1016/j.ifset.2016.10.010.

Al-nemrawi, N.K., Alsharif, S.S.M., Dave, R.H., 2018. Preparation of chitosan-tpp nanoparticles: the influence of chitosan polymeric properties and formulation variables. Int. J. App. Pharm. 10 (5), 60. https://doi.org/10.22159/ijap.2018v10i5.26375.

Al-Nemrawi, N., Alshraiedeh, N., Zayed, A., Altaani, B., 2018. Low molecular weight chitosan-coated PLGA nanoparticles for pulmonary delivery of tobramycin for cystic fibrosis. Pharmaceuticals (Basel) 11 (1), 28. https://doi.org/10.3390/ph11010028.

Al-Nemrawi, N.K., Dave, R.H., 2016. Formulation and characterization of acetaminophen nanoparticles in orally disintegrating films. Drug Deliv. 23 (2), 540–549. https://doi.org/10.3109/10717544.2014.936987.

Azam, A., Ahmed, A.S., Oves, M., Khan, M.S., Habib, S.S., Memic, A., 2012. Antimicrobial activity of metal oxide nanoparticles against Gram-positive and Gram-negative bacteria: a comparative study. Int. J. Nanomed. 7, 6003–6009. https://doi.org/10.2147/IJN.S35347.

Azizi-Lalabadi, M., Ehsani, A., Divband, B., Alizadeh-Sani, M., 2019. Antimicrobial activity of Titanium dioxide and Zinc oxide nanoparticles supported in 4A zeolite and evaluation the morphological characteristic. Sci. Rep. 9, 17439. https://doi.org/10.1038/s41598-019-54025-0.

Beveridge, T.J., 1999. Structures of gram-negative cell walls and their derived membrane vesicles. J. Bacteriol. 181 (16), 4725–4733. https://doi.org/10.1128/JB.181.16.4725-4733.1999.

Bharathi, D., Ranjithkumar, R., Chandarshekar, B., Bhuvaneshwari, V., 2019. Preparation of chitosan coated zinc oxide nanocomposite for enhanced antibacterial and photocatalytic activity: as a bionanocomposite. Int. J. Biol. Macromol. 129, 989–996. https://doi.org/10.1016/j.ijbiomac.2019.02.061.

Cheow, W.S., Chang, M.W., Hadinoto, K., 2010. Antibacterial efficacy of inhalable levofloxacin-loaded polymeric nanoparticles against E. coli biofilm cells: the effect of antibiotic release profile. Pharm. Res. 27 (8), 1597–1609. https://doi.org/10.1007/s11095-010-0142-6.

Davis, B.D., 1987. Mechanism of bactericidal action of aminoglycosides. Microbiol. Rev. 51 (3), 341–350.

El-Alfy, E.A., El-Bisi, M.K., Taha, G.M., Ibrahim, H.M., 2020. Preparation of biocompatible chitosan nanoparticles loaded by tetracycline, gentamycin and ciprofloxacin as novel drug delivery system for improvement the antibacterial

properties of cellulose based fabrics. Int. J. Biol. Macromol. 161, 1247–1260. https://doi.org/10.1016/j.ijbiomac.2020.06.118.
Grenha, A., 2012. Chitosan nanoparticles: a survey of preparation methods. J. Drug Target. 20 (4), 291–300. https://doi.org/10.3109/1061186X.2011.654121.
Gutha, Y., Pathak, J.L., Zhang, W., Zhang, Y., Jiao, X., 2017. Antibacterial and wound healing properties of chitosan/poly(vinyl alcohol)/zinc oxide beads (CS/PVA/ZnO). Int. J. Biol. Macromol. 103, 234–241. https://doi.org/10.1016/j.ijbiomac.2017.05.020.
Infrared Spectroscopy Absorption Table [WWW Document], 2014. Chemistry LibreTexts. URL https://chem.libretexts.org/Ancillary_Materials/Reference/Reference_Tables/Spectroscopic_Parameters/Infrared_Spectroscopy_Absorption_Table (accessed 10.21.21).
IR Spectrum Table [WWW Document], n.d. URL https://www.sigmaaldrich.com/JO/en/technical-documents/technical-article/analytical-chemistry/photometry-and-reflectometry/ir-spectrum-table (accessed 10.15.21).
Janaki, A.C., Sailatha, E., Gunasekaran, S., 2015. Synthesis, characteristics and antimicrobial activity of ZnO nanoparticles. Spectrochim. Acta Part A Mol. Biomol. Spectrosc. 144, 17–22. https://doi.org/10.1016/j.saa.2015.02.041.
Jonassen, H., Kjøniksen, A.-L., Hiorth, M., 2012. Effects of ionic strength on the size and compactness of chitosan nanoparticles. Colloid Polym. Sci. 290 (10), 919–929. https://doi.org/10.1007/s00396-012-2604-3.
Junejo, Y., Safdar, M., Akhtar, M.A., Saravanan, M., Anwar, H., Babar, M., Bibi, R., Pervez, M.T., Hussain, T., Babar, M.E., 2019. Synthesis of tobramycin stabilized silver nanoparticles and its catalytic and antibacterial activity against pathogenic bacteria. J. Inorg. Organomet. Polym. Mater. 29 (1), 111–120. https://doi.org/10.1007/s10904-018-0971-z.
Kashi, T.S.J., Eskandarion, S., Esfandyari-Manesh, M., Marashi, S.M.A., Samadi, N., Fatemi, S.M., Atyabi, F., Eshraghi, S., Dinarvand, R., 2012. Improved drug loading and antibacterial activity of minocycline-loaded PLGA nanoparticles prepared by solid/oil/water ion pairing method. Int. J. Nanomed. 7, 221–234. https://doi.org/10.2147/IJN.S27709.
Khan, S.A., Shahid, S., Mahmood, T., Lee, C.-S., 2021. Contact lenses coated with hybrid multifunctional ternary nanocoatings (Phytomolecule-coated ZnO nanoparticles: Gallic Acid:Tobramycin) for the treatment of bacterial and fungal keratitis. Acta Biomater. 128, 262–276. https://doi.org/10.1016/j.actbio.2021.04.014.
Kumar, S.S., Venkateswarlu, P., Rao, V.R., Rao, G.N., 2013. Synthesis, characterization and optical properties of zinc oxide nanoparticles. Int. Nano Lett. 3, 30. https://doi.org/10.1186/2228-5326-3-30.
Kumari, S., Rath, P.K., 2014. Extraction and characterization of chitin and chitosan from (Labeo rohit) fish scales. Procedia Mater. Sci. 6, 482–489. https://doi.org/10.1016/j.mspro.2014.07.062.
La, D.D., Nguyen-Tri, P., Le, K.H., Nguyen, P.T.M., Nguyen, M.-B., Vo, A.T.K., Nguyen, M.T.H., Chang, S.W., Tran, L.D., Chung, W.J., Nguyen, D.D., 2021. Effects of antibacterial ZnO nanoparticles on the performance of a chitosan/gum arabic edible coating for post-harvest banana preservation. Prog. Org. Coat. 151, 106057. https://doi.org/10.1016/j.porgcoat.2020.106057.
Lawrie, G., Keen, I., Drew, B., Chandler-Temple, A., Rintoul, L., Fredericks, P., Grøndahl, L., 2007. Interactions between alginate and chitosan biopolymers characterized using FTIR and XPS. Biomacromolecules 8 (8), 2533–2541. https://doi.org/10.1021/bm070014y.
Laxer, R.M., Mackay, E., Marks, M.I., 1975. Antibacterial activity of tobramycin against gram-negative bacteria and the combination of ampicillin/tobramycin against E. coli. Chemotherapy 21, 90–98. https://doi.org/10.1159/000221851.
Lister, P.D., Wolter, D.J., Hanson, N.D., 2009. Antibacterial-resistant Pseudomonas aeruginosa: clinical impact and complex regulation of chromosomally encoded resistance mechanisms. Clin. Microbiol. Rev. 22 (4), 582–610. https://doi.org/10.1128/CMR.00040-09.
Lüderitz, O., Freudenberg, M.A., Galanos, C., Lehmann, V., Rietschel, E.T., Shaw, D.H., 1982. Lipopolysaccharides of Gram-Negative Bacteria. In: Bronner, F., Kleinteller, A. (Eds.), Current Topics in Membranes and Transport, Membrane Lipids of Prokaryotes. Academic Press, pp. 79–151. https://doi.org/10.1016/S0070-2161(08)60309-3.
Medina, E., Pieper, D.H., 2016. Tackling threats and future problems of multidrug-resistant bacteria. Curr. Top. Microbiol. Immunol. 398, 3–33. https://doi.org/10.1007/82_2016_492.
Mohan, A.C., Renjanadevi, B., 2016. Preparation of zinc oxide nanoparticles and its characterization using scanning electron microscopy (SEM) and X-ray diffraction(XRD). Procedia Technol. 24, 761–766. https://doi.org/10.1016/j.protcy.2016.05.078.
Motelica, L., Popescu, A., Răzvan, A.-G., Oprea, O., Truşcă, R.-D., Vasile, B.-S., Dumitru, F., Holban, A.-M., 2020. Facile use of ZnO nanopowders to protect old manual paper documents. Materials 13, 5452. https://doi.org/10.3390/ma13235452.
Nazoori, E.S., Kariminik, A., 2018. In vitro evaluation of antibacterial properties of zinc oxide nanoparticles on pathogenic prokaryotes. J. Apple Biotechnol. Rep. 5, 162–165 https://doi.org/10.29252/JABR.05.04.05.
Nguyen, N.T., Nguyen, N.T., Nguyen, V.A., 2020. In situ synthesis and characterization of ZnO/chitosan nanocomposite as an adsorbent for removal of Congo red from aqueous solution. Adv. Polym. Tech. 2020, 1–8. https://doi.org/10.1155/2020/3892694.
Nguyen, T.V., Nguyen, T.T.H., Wang, S.-L., Vo, T.P.K., Nguyen, A.D., 2017. Preparation of chitosan nanoparticles by TPP ionic gelation combined with spray drying, and the antibacterial activity of chitosan nanoparticles and a chitosan nanoparticle–amoxicillin complex. Res. Chem. Intermed. 43 (6), 3527–3537. https://doi.org/10.1007/s11164-016-2428-8.
Radulescu, M., Ficai, D., Oprea, O., Ficai, A., Andronescu, E., Holban, M., 2015. Antimicrobial chitosan based formulations with impact on different biomedical applications. Curr. Pharm. Biotechnol. 16, 128–136.
Raghupathi, K.R., Koodali, R.T., Manna, A.C., 2011. Size-dependent bacterial growth inhibition and mechanism of antibacterial activity of zinc oxide nanoparticles. Langmuir 27 (7), 4020–4028. https://doi.org/10.1021/la104825u.
Raja, K., Ramesh, P.S., Geetha, D., 2014. Structural, FTIR and photoluminescence studies of Fe doped ZnO nanopowder by co-precipitation method. Spectrochim. Acta A Mol. Biomol. Spectrosc. 131, 183–188. https://doi.org/10.1016/j.saa.2014.03.047.
Rizvi, S.A.A., Saleh, A.M., 2018. Applications of nanoparticle systems in drug delivery technology. Saudi Pharm. J. 26 (1), 64–70. https://doi.org/10.1016/j.jsps.2017.10.012.
Russ, H., McCleary, D., Katimy, R., Montana, J.L., Miller, R.B., Krishnamoorthy, R., Davis, C.W., 1998. Development and validation of a stability-indicating HPLC method for the determination of tobramycin and its related substances in an ophthalmic suspension. J. Liq. Chromatogr. Relat. Technol. 21 (14), 2165–2181. https://doi.org/10.1080/10826079808006616.
Sanpui, P., Murugadoss, A., Prasad, P., Ghosh, S., Chattopadhyay, A., 2008. The antibacterial properties of a novel chitosan-Ag-nanoparticle composite. Int. J. Food Microbiol. 124 (2), 142–146. https://doi.org/10.1016/j.ijfoodmicro.2008.03.004.
Scolari, I.R., Páez, P.L., Musri, M.M., Petiti, J.P., Torres, A., Granero, G.E., 2020. Rifampicin loaded in alginate/chitosan nanoparticles as a promising pulmonary carrier against Staphylococcus aureus. Drug Deliv. Transl. Res. 10 (5), 1403–1417. https://doi.org/10.1007/s13346-019-00705-3.
Sekhri, K., n.d. Antimicrobial Resistance: Understanding Solutions and Future Developments.
Shadomy, S., Kirchoff, C., 1972. In vitro susceptibility testing with tobramycin. Antimicrob. Agents Chemother. 1 (5), 412–416. https://doi.org/10.1128/AAC.1.5.412.
Siddiqi, K.S., ur Rahman, A., Tajuddin, Husen, A., 2018. Properties of zinc oxide nanoparticles and their activity against microbes. Nanoscale Res. Lett. 13 (1). https://doi.org/10.1186/s11671-018-2532-3.
Moore, B.S., Carter, G.T., Brönstrup, M., 2017. Editorial: are natural products the solution to antimicrobial resistance? Nat. Prod. Rep. 34 (7), 685–686. https://doi.org/10.1039/C7NP90026K.
Sobhani, Z., Mohammadi Samani, S., Montaseri, H., Khezri, E., 2017. Nanoparticles of chitosan loaded ciprofloxacin: fabrication and antimicrobial activity. Adv. Pharm. Bull. 7, 427–432 https://doi.org/10.15171/apb.2017.051.
Sondi, I., Salopek-Sondi, B., 2004. Silver nanoparticles as antimicrobial agent: a case study on E. coli as a model for Gram-negative bacteria. J. Colloid Interface Sci. 275, 177–182. https://doi.org/10.1016/j.jcis.2004.02.012.
Szymańska, E., Winnicka, K., 2015. Stability of chitosan—a challenge for pharmaceutical and biomedical applications. Mar. Drugs 13, 1819–1846. https://doi.org/10.3390/md13041819.
Vaezifar, S., Razavi, S., Golozar, M.A., Karbasi, S., Morshed, M., Kamali, M., 2013. Effects of some parameters on particle size distribution of chitosan nanoparticles prepared by ionic gelation method. J. Clust. Sci. 24 (3), 891–903. https://doi.org/10.1007/s10876-013-0583-2.
Yadav, S., Mehrotra, G.K., Dutta, P.K., 2021. Chitosan based ZnO nanoparticles loaded gallic-acid films for active food packaging. Food Chem. 334, 127605. https://doi.org/10.1016/j.foodchem.2020.127605.
Yusof, N.A.A., Zain, N.M., Pauzi, N., 2019. Synthesis of ZnO nanoparticles with chitosan as stabilizing agent and their antibacterial properties against Gram-positive and Gram-negative bacteria. Int. J. Biol. Macromol. 124, 1132–1136. https://doi.org/10.1016/j.ijbiomac.2018.11.228.